Paramagnetic NH_3Cl and NH_3Br Color Centers in Irradiated Ammonium Halide Single Crystals

FRANK W. PATTEN
U. S. Naval Research Laboratory, Washington, D. C. 20390
(Received 19 June 1968)

Radiation-induced NH_3Cl and NH_3Br defect centers have been studied in ammonium halide single crystals by EPR and optical spectroscopy. The defects are most likely formed by removal of H^0 from an ammonium ion with subsequent bonding of NH_3^+ to X^- along a ⟨111⟩ direction. In the NH_3Cl center, NH_3^+ is a nearly planar group loosely bonded to a Cl^-; in the NH_3Br center there is more tendency toward sp^3 hybridization of the N orbitals, and stronger covalency within the nitrogen-halogen bond. The molecular orbital description of these centers shows a strong similarity to that of mixed V_K color centers in the alkali halides. Optical absorptions due to the NH_3Cl and NH_3Br centers were observed at 3.31 and 3.14 eV, respectively. The NH_3Cl defects were observed to undergo thermally induced reorientations which are strongly influenced by the ordering of the surrounding ammonium ions at low temperature.

INTRODUCTION

THE ammonium halides are a suitable system for the extension of studies of radiation-induced color centers which have in the past been studied primarily in the alkali halides.[1] Recent electron-paramagnetic-resonance and optical-absorption experiments in the ammonium halides have led to the identification of two color centers which are also found in the alkali halides: (1) the F center, which is an electron trapped at a negative ion vacancy[2]; (2) the V_K center, a hole shared by two nearest-neighbor halide ions.[3,4] A third center has been identified as NH_3X, where X represents a halogen atom.[5,6] In this paper we give a fuller description of the structure of this center in ammonium chloride, deuterated ammonium chloride, and ammonium bromide single crystals. The kinetics of the reorientation behavior, dealt with briefly here, will be described more completely in a subsequent publication.[7]

CRYSTAL STRUCTURE

Both NH_4Cl and NH_4Br have the CsCl structure at room temperature,[8] as shown in Fig. 1. Below 242.8°K in the chloride, 234.5°K in the bromide, both materials undergo a λ transition of the order-disorder type involving the relative orientations of adjacent ammonium ions within the lattice.[9] The tetrahedral NH_4^+ ions can be oriented in two equivalent positions of minimum electrostatic potential within the cube of nearest-neighbor halide ions. In the completely ordered state of NH_4Cl, all NH_4^+ ions have the same relative orientation, for a given domain, with respect to the crystallographic axes; the space-group symmetry is $T_d^1(P\bar{4}3m)$. ND_4Cl has similar structural changes. The NH_4Br crystal structure becomes tetragonal below the λ point, though this is the result of a slight change of 0.4% of the lattice parameter along one cube direction. Additionally, the Br^- ions are displaced about 3.0% from planes perpendicular to the distortion axis, lying alternately in positive and negative directions along the tetragonal axis. The space-group symmetry is $D_{4h}^7(P/nmm)$. In the ordered NH_4Br crystal, adjacent NH_4^+ ions in a plane perpendicular to the distortion axis have opposite orientations, and have the same orientation along the distortion axis. In both phases of both materials the NH_4^+ ions execute torsional oscillations (librations) about their equilibrium positions.[10]

The experiments reported here deal with the low-temperature, ordered phases of these materials.

EXPERIMENTAL PROCEDURE

Crystal growth, experimental equipment, and irradiation techniques have been described in a previous paper.[3] Deuterated single crystals were prepared by dissolving analytical grade NH_4Cl and urea in 99.85 mole% D_2O and evaporating to dryness four times before growing

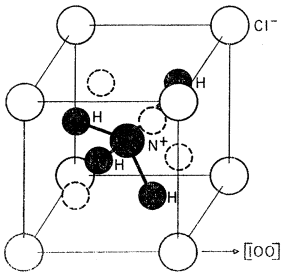

FIG. 1. Unit cell for an NH_4Cl single crystal in the ordered phase, with the alternative positions of the hydrogen atoms (dashed circles) which can be occupied above the transition temperature (−30°C).

[1] J. H. Schulman and W. D. Compton, *Color Centers in Solids* (The Macmillan Co., New York, 1962).
[2] F. W. Patten, Solid State Commun. 6, 65 (1968).
[3] F. W. Patten and M. J. Marrone, Phys. Rev. 142, 513 (1966).
[4] H. R. Zeller, L. Vannotti, and W. Kanzig, Physik Kondensierten Materie 2, 133 (1964).
[5] F. W. Patten, Phys. Letters 21, 277 (1966); in *Proceedings of the XIVth Colloque Ampère* (North-Holland Publishing Co., Amsterdam, 1967).
[6] L. Vannotti, H. R. Zeller, K. Bachmann, and W. Kanzig, Physik Kondensierten Materie 6, 51 (1967).
[7] F. W. Patten (to be published).
[8] R. W. G. Wyckoff, *Crystal Structures* (Interscience Publishers, Inc., New York, 1951), Vol. I.
[9] H. A. Levy and S. W. Peterson, Phys. Rev. 86, 766 (1952).
[10] The evidence for these statements has been reviewed in the articles by C. W. Garland *et al.* [J. Chem. Phys. 44, 1112 (1966); J. Phys. Chem. Solids 28, 799 (1967)].

crystals in a temperature-regulated solution; it is expected that 99.0% deuteration was achieved. EPR measurements were made with X-band (9 kMc/sec) and K-band (25 kMc/sec) superheterodyne spectrometers of conventional design as well as a Varian E-3 X-band spectrometer with 100-kc/sec detection. Computed spectra were obtained using a Control Data Corporation 3800 computer and graphical plotter. Optical measurements were made with a Cary model 14 MR recording spectrophotometer.

RESULTS

1. 77°K EPR Spectra

Single crystals of NH_4Cl, ND_4Cl, and NH_4Br at 77°K were irradiated with x rays for 1–2 h. The crystals were oriented with an estimated accuracy of $\pm 1°$ by using the V_K center EPR spectrum as a reference, since it is known to have its principal axes exactly aligned along the ⟨100⟩ cubic axes.[3] V_K centers were then eliminated either by bleaching into their optical absorption bands or by thermally cycling the sample between 77 and about 150°K. The remaining EPR spectrum in each material was found to be due to a single species with several magnetically inequivalent sites. The anisotropic hyperfine spectrum indicated a major symmetry axis for each center along a ⟨111⟩ direction. Spectra are shown in Fig. 2 for the applied magnetic field parallel to a ⟨100⟩ direction, where the different orientations become magnetically equivalent.

We may interpret these spectra by the following simple reasoning. Assume the paramagnetic species to be the same in each crystal (with appropriate substitution of Br for Cl and D for H). The four groups of hyperfine lines in the top spectrum suggest a dominant interaction of an unpaired electron with one Br nucleus of spin $\frac{3}{2}$ (double intergration shows that the four absorptions have approximately equal areas). If interactions with the D nuclei in the deuterated center can be assumed to contribute only to the linewidth, an excellent fit is obtained to the middle spectrum by postulating an equivalent interaction with one N nucleus ($I=1$) and one Cl nucleus ($I=\frac{3}{2}$). The bottom spectrum can be constructed by taking additional interactions with three H nuclei (inequivalent for this orientation of the applied magnetic field). The simplest paramagnetic center having these collective properties is NH_3X (X=halogen atom). This defect would arise by the removal of a hydrogen atom from an NH_4^+ group, with subsequent formation of an N—X bond along ⟨111⟩ with one of the surrounding cubic array of halide ions.

In order to form an idea of the bonding situation, we consider an intermediate state after removal of the H atom from the NH_4^+ group by the incident radiation. The NH_3^+ ion is planar when unassociated with other atoms, with an unpaired electron in the nitrogen $2p$ orbital perpendicular to the plane.[11] Covalent bonding with the halide ion X^- will occur through overlap of $N^+(2p_z)^1$ and $X^-(np_z)^2$ orbitals. The two linear combinations obtained from these atomic orbitals represent

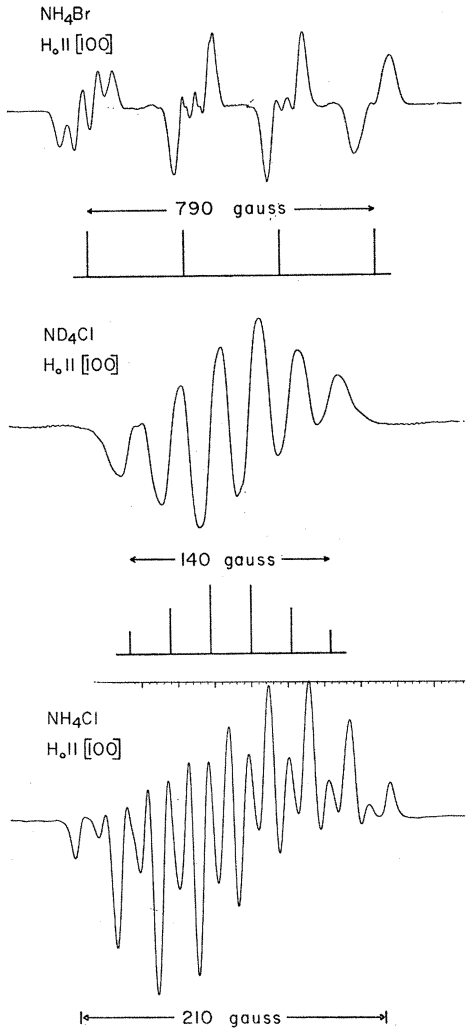

FIG. 2. EPR spectra (dx''/dH) observed in single crystals of NH_4Br, ND_4Cl, and NH_4Cl irradiated at 77°K with x rays, after suitable optical bleaching or thermal cycling (see text). $\nu_0=9.4$ kMc/sec, $T=77$°K.

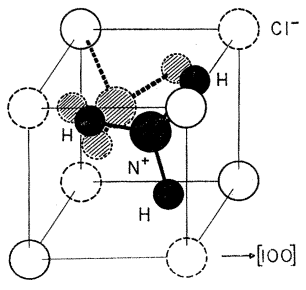

FIG. 3. Structural representation of the NH_3Cl defect center. Dashed circles for Cl^- indicate the ions which do not interact with the reorienting NH_3^+. Another orientation of NH_3^+ is shown.

[11] This has been observed as a stable defect at room temperature in irradiated NH_4ClO_4 by T. Cole [J. Chem. Phys. 35, 1169 (1961)].

TABLE I. NH_3Cl hyperfine interactions (in G) for different field orientations ($A_{Cl^{37}}=0.83237\,A_{Cl^{35}}$; linewidth=6 G).

Field orientation	Angle with N—Cl bond, Θ	$A_{Cl^{35}}$	A_N	A_{H_a}	A_{H_b}	A_{H_c}
$\mathbf{H}\|\langle 111\rangle$	0°: 1 site 70.5°: 3 sites	43.3	46.5	25.0	25.0	25.0
$\mathbf{H}\|\langle 110\rangle$	35.2°: 2 sites 90°: 2 sites	36.0	38.5	27.5	27.5	21.5
$\mathbf{H}\|\langle 100\rangle$	54.7°: 4 sites	27.5	28.0	28.0	28.0	15.0

a lower energy bonding σ orbital (doubly occupied) and a higher energy antibonding σ orbital (singly occupied). Thus the unpaired electron can be expected to lie largely in the antibonding σ orbital along the N—X bond axis.

A model for the stationary NH_3Cl defect[12] is depicted in Fig. 3. The N—H bonds are directed toward Cl^- ions adjacent to the Cl which is part of the defect. For an approximately planar NH_3 group the N—Cl bond length within this undistorted model would measure about 2 Å, which is similar to the C—Cl bond length in the nearly isoelectronic CH_3Cl molecule. Another possible orientation for the defect differs from the former by a 60° rotation about the N—Cl axis. In both cases the N—H bonds lie in the {110} planes, and the EPR spectra are not magnetically distinguishable. Since inversion of the coordinates of the defect through the center of the unit cell does not produce a magnetically distinct center, there is one distinct center for each body diagonal of the unit cube, and therefore four inequivalent sites for a generally oriented magnetic field. All sites become magnetically equivalent when the field is oriented along a cubic axis.

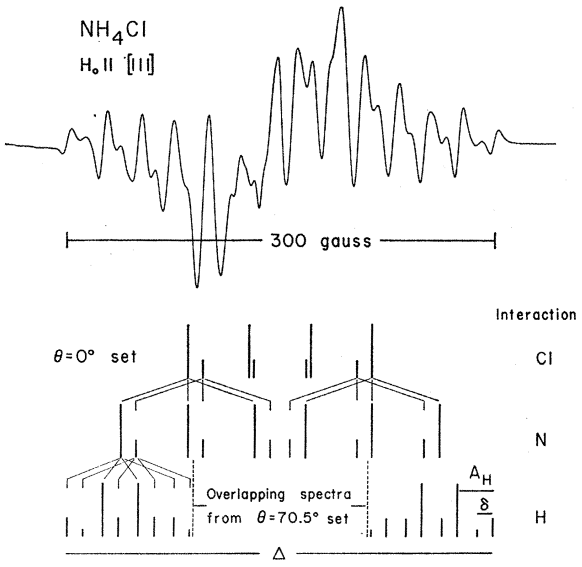

FIG. 4. EPR spectrum for the NH_3Cl defect center for $\mathbf{H}\|[111]$.

[12] Reorientations at this temperature occur in a time long compared to the inverse of the rigid-lattice linewidth.

(*a*) *NH_3Cl Center.* Because of the high degree of overlapping of EPR transitions (there are 192 first-order transitions for each site), it was not possible to observe unambiguously the angular variation of individual hyperfine lines with magnetic field direction in a given plane. Hyperfine interactions were measured with the field along directions for which some of the sites became equivalent and resolution was improved. The orientation most convenient for analysis of the spectra is the one with the field along the N—Cl bond of one site. Such a spectrum is shown in Fig. 4, where the hyperfine interactions (A_{Cl} and A_N) of the unpaired electron with the Cl and N nuclei are largest and the three H nuclei have equivalent interactions (A_H). There are two Cl isotopes of spin $\frac{3}{2}$ each, Cl^{35} and Cl^{37}, with relative abundances of 75 and 25% and magnetic moments (μ) of 0.82091 and 0.68330 μ_N, respectively. Hyperfine transitions due to the different Cl isotopes are easily distinguishable and the measurement of their separation, δ, provides the best means of determining the Cl hyperfine interaction. Other quantities which can be determined with relative precision are the proton interaction A_H and the spectrum width Δ, as shown in Fig. 4. The Cl and N hyperfine interactions are then found from the relations[13]

$$A_{Cl}35=3.977\delta,\quad A_N=\tfrac{1}{2}(\Delta-3A_H-11.931\delta).$$

Using values for the nuclear hyperfine interactions obtained in this way, an excellent fit was obtained to that part of the observed spectrum due to only the [111]-oriented center (the construction at the bottom of Fig. 4 is incomplete, for clarity).

Nuclear hyperfine interaction constants were also obtained for $\mathbf{H}\|[110]$ for the two sites for which the angle Θ of the field to the N—Cl bond is 35.2°, and $\mathbf{H}\|[100]$, where Θ is 54.7° for all sites. Measurement errors became greater as Θ was increased to the point where all sites became equivalent. A computer program which would graphically simulate recorded EPR spectra was devised[14] to overcome some of the uncertainties in line positions due to overlapping transitions. Given the initial hyperfine constants and linewidth, the computer summed over first derivatives of Gaussian envelopes at the expected line positions and plotted the resulting spectrum. A routine was also included which would vary the initial parameters to produce a least-squares fit of the computed spectrum to selected data points, usually the derivative extrema. This resulted in some changes in the initial parameters for cases where Θ was large, with an improved fit of the computed spectrum to the recorded spectrum. The values of the hyperfine constants obtained from the best fit for each orientation are given in Table I.

[13] Because of the difficulty in distinguishing overlapping lines, errors were made in the initial evaluation of the hyperfine interactions for this center (Refs. 5 and 6).

[14] Computer program written by C. L. Marquardt of this laboratory.

TABLE II. Spin Hamiltonian parameters for NH_3Cl, ND_3Cl, and NH_3Br, compared with results for NH_3^+ and Cl_2^-, Br_2^-.

Tensor components	NH_3Cl	(From 180°K results)	ND_3Cl	NH_3Br	NH_3^+ [a]	Cl_2^- [b]	Br_2^- [b]
$A_\parallel(Cl^{35},Br^{79})$ (G)	$+43.3\pm0.8$	···	$+43\pm3$	$+426.4\pm1$		±101.3	$+450.0$
$A_\perp(Cl^{35},Br^{79})$ (G)	$+13.5\pm2$	14.5 ± 1	$+15\pm4$	$+106\pm5$		$+12.5$	$+79$
$A_\parallel(N)$ (G)	$+46.5\pm0.8$	···	$+46\pm3$	$+51.5\pm1$	$+44.6$		
$A_\perp(N)$ (G)	$+9.0\pm4$	8.0 ± 1	$+10\pm5$	$+36\pm5$	$+10, +3.8$		
$Q'(Cl^{35},Br^{79})$ (G)	···	···	···	30 ± 10		9	40
A(H) (G)	-7.8 ± 3	4.0 ± 1	$\psi=(93\pm2)°$		-5.4		
B(H) (G)	-25.0 ± 1	25.0 ± 1		$A_H(\mathbf{H}\|\|[111])=16\pm1$	-29.6		
C(H) (G)	-37.2 ± 3	34.0 ± 1			-47.1		
$g_\parallel$	2.0019 ± 0.0002	···	2.0020 ± 0.0004	1.9954 ± 0.0002		2.0012	1.9833
$g_\perp$	2.0079 ± 0.0005	···	2.0080 ± 0.0010	2.0596 ± 0.0010		2.0426	2.169

[a] M. Fujimoto and J. R. Morton, Can. J. Chem. 43, 1012 (1965).
[b] T. G. Castner and W. Kanzig, J. Phys. Chem. Solids 3, 178 (1957); D. Schoemaker, Phys. Rev. 149, 693 (1966).

The EPR transitions can be obtained from the spin Hamiltonian

$$\mathcal{H}=\mu_B\mathbf{H}\cdot\mathbf{g}\cdot\mathbf{S}+\mathbf{S}\cdot\sum_i \mathbf{A}_i\cdot\mathbf{I}_i-g_n\mu_N\mathbf{H}\cdot\sum_i \mathbf{I}_i, \quad (1)$$

where we have neglected the effects of the halogen quadrupole moment. The last term in the Hamiltonian (1) is the nuclear Zeeman energy. This term applies particularly to the hydrogen nuclei, and is of little importance for the other nuclei. Two principal axis systems, shown in Fig. 5, are required to diagonalize the hyperfine tensors $\mathbf{A}_i$. Since the symmetry of the NH_3Cl center and its environment is C_{3V}, the g tensor and the Cl and N hyperfine tensors are expected to have axial symmetry about ⟨111⟩, which is observed within experimental error. Principal axes for the proton interactions were chosen in the usual way for an α hydrogen.[15] Bleaney[16] has derived the formula for the angular dependence of $\Delta M_S=\pm1$, $\Delta m_I=0$ transitions for an axial spin Hamiltonian of a single atom, to second order in the hyperfine interactions. We apply these results to the N and Cl interactions in the above Hamiltonian, within an excellent approximation. Additional terms involving the product of magnetic quantum numbers for the different nuclei, largest for the ⟨100⟩ directions, are of the order of $0.15m_im_j$ G and may therefore be dismissed. Diagonal values of the g tensor and hyperfine tensors for Cl and N are given in Table II.

In the principal axis system of the protons, the hyperfine interactions have the form

$$\mathcal{H}_i^{hf}=h(A_iS_zI_{iz}+B_iS_xI_{ix}+C_iS_yI_{iy}). \quad (2)$$

The $\Delta M_S=\pm1$, $\Delta m_I=0$ transitions, for an arbitrary orientation of the field, are given by[17]

$$\Delta\nu=(A^2\cos^2\theta+B^2\sin^2\theta\cos^2\varphi+C^2\sin^2\theta\sin^2\varphi)^{1/2}m_I, \quad (3)$$

where $\Delta\nu$ is the frequency shift of the hyperfine transitions, m_I is the projection of the nuclear spin on the magnetic field due to the electron, and θ and φ are the polar and azimuthal angles specifying the orientation of the external magnetic field in the principal axis coordinate system. We evaluate Eq. (3) for the field orientations for which data were taken. With the configuration shown in Fig. 5, for an arbitrary angle ψ between N—Cl and N—H bonds, and assuming only that the N—H bonds lie in {110} planes, the hyperfine transitions for the three field directions are as follows:

1. $\mathbf{H}\|[111]$, case of $\mathbf{H}$ at 0° to the N—Cl bond,

$$\Delta\nu_{Ha,b,c}=[A^2\cos^2\psi+B^2\sin^2\psi]^{1/2}m_I; \quad (4)$$

2. $\mathbf{H}\|[110]$, case of $\mathbf{H}$ at 35.2° to the N—Cl bond,

$$\Delta\nu_{Ha,b}=[\tfrac{1}{6}A^2(a+b)^2+\tfrac{1}{12}B^2(2a-b)^2+\tfrac{1}{4}C^2]^{1/2}m_I, \quad (5)$$

$$\Delta\nu_{Hc}=[\tfrac{2}{3}a^2(A^2-B^2)+B^2]^{1/2}m_I; \quad (6)$$

3. $\mathbf{H}\|[100]$, $\mathbf{H}$ at 54.7° to the N—Cl bond,

$$\Delta\nu_{Ha,b}=[\tfrac{1}{3}A^2a^2+\tfrac{1}{6}B^2b^2+\tfrac{1}{2}C^2]^{1/2}m_I, \quad (7)$$

$$\Delta\nu_{Hc}=[\tfrac{1}{3}A^2b^2+\tfrac{2}{3}B^2a^2]^{1/2}m_I, \quad (8)$$

where

$$a=-\cos\psi+(2)^{-1/2}\sin\psi, \qquad b=-\cos\psi-(2)^{1/2}\sin\psi. \quad (9)$$

In each case, sites having the same N—Cl bond angle with the field have equivalent proton interactions. Equations (4)–(9) can be simultaneously solved to give the principal values for the hyperfine interaction and the angle ψ, which is about 93° for NH_3Cl. The results are presented in Table II.

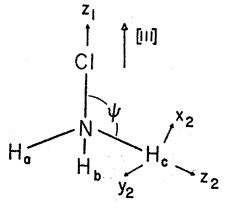

FIG. 5. Principal axis systems for the NH_3X defect center.

[15] T. Cole, C. Heller, and H. M. McConnell, Proc. Natl. Acad. Sci. 45, 525 (1959).
[16] B. Bleaney, Phil. Mag. 42, 441 (1951).
[17] E. L. Cochran, F. J. Adrian, and V. A. Bowers, J. Chem. Phys. 34, 255 (1961).

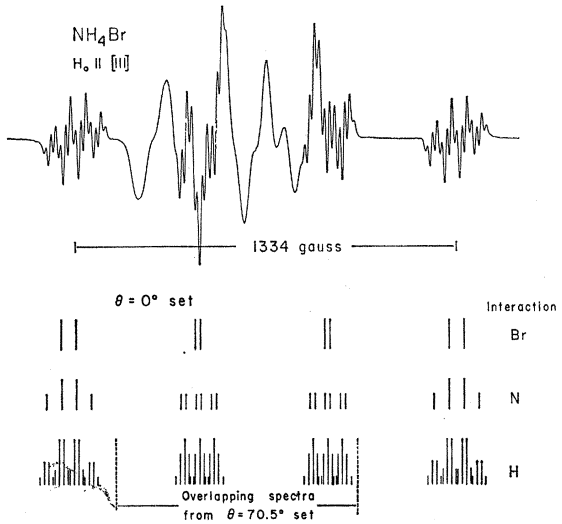

FIG. 6. EPR spectrum for the NH_3Br defect center for $\mathbf{H}\|[111]$.

For comparison, the diagonal hyperfine and g-tensor data are given in Table II for the NH_3^+ and X_2^- paramagnetic centers. The NH_3^+ center, which is stable even at room temperature, was shown by Cole[11] and by Fujimoto and Morton[18] to be a planar π-electron radical with negative spin density on the α protons, in accord with theory.[19] It is seen from the table that the NH_3^+ defect and this portion of the NH_3Cl center are very similar. An analysis, in the next section, of the reorienting NH_3Cl defect shows that the components of the N and H hyperfine tensors, individually, must have the same signs. Accordingly, these signs are taken to be those of the NH_3^+ defect. The halogen hyperfine tensor signs are similarly obtained from the X_2^- center, since it will later be seen that the NH_3X electronic structure is similar to that of the XY^- mixed V_K center.

For some orientations of the field, notably $\mathbf{H}\|[100]$, it was not possible to obtain an accurate fit of the computed spectrum to the recorded data. At higher frequencies (K band) the fit was much worse with many new absorption lines, unaccountable by the theory presented, appearing in the spectrum. This discrepancy is attributed to the existence of "forbidden" transitions involving the sinultaneous reorientation of the electron and proton spin, $\Delta M_S=\pm1$, $\Delta m_I=\pm1$. Transitions of this type are due to the presence in the Hamiltonian of nuclear Zeeman and hyperfine terms of the same order of magnitude which compete in aligning the nuclear spin. These transitions have been investigated in the similar case of an α hydrogen in a C—H bond[19,20]; they have also been treated more generally.[21]

[18] M. Fujimoto and J. R. Morton, Can. J. Chem. 43, 1012 (1965).

[19] H. M. McConnell, C. Heller, T. Cole, and R. W. Fessenden, J. Am. Chem. Soc. 82, 766 (1960).

[20] I. Miyagawa and W. Gordy, J. Chem. Phys. 32, 255 (1960).

[21] J. A. Weil and J. H. Anderson, J. Chem. Phys. 35, 1410 (1961).

We may determine the expected intensity $\mathcal{I}$ of the $\Delta m_I=\pm1$ transitions relative to the $\Delta m_I=0$ transitions by obtaining the nondiagonal matrix of hyperfine components for rotated axes appropriate to a particular field direction. For the field direction $\mathbf{H}\|[100]$, the orthogonal rotation matrix for one hydrogen is

$$\mathbf{R}_\alpha=\frac{1}{\sqrt{6}}\begin{bmatrix}-b & -\sqrt{3} & \sqrt{2}a\\ 2a & a & \sqrt{2}b\\ -b & \sqrt{3} & \sqrt{2}a\end{bmatrix},$$

where a and b are given by Eq. (9); the new axes are chosen along the cubic directions. The rotation matrices for the other two hydrogens are obtained by permutation of the rows. The hyperfine matrix in the new representation is obtained by applying the orthogonal transformation $\mathbf{R}_\alpha\mathbf{A}\mathbf{R}_\alpha^T$. Using Eq. (18) of the treatment by Miyagawa and Gordy,[20] one finds that at a resonance frequency of 9.1 KMc, $\mathcal{I}(\Delta m_I=\pm1)/\mathcal{I}(\Delta m_I=0)\cong1/50$, and at a resonance frequency of 24.5 KMc, $\mathcal{I}(\Delta m_I=\pm1)/\mathcal{I}(\Delta m_I=0)\cong\frac{1}{3}$, for one of the hydrogens. The intensity of the forbidden transitions for the other two H nuclei is smaller by an order of magnitude. This is in accord with observations. The angular dependence of the forbidden transitions is a result of the change in magnitude of off-diagonal elements of the hyperfine tensor with a change of field direction; of the three directions examined, off-diagonal elements are largest for $\mathbf{H}\|[100]$, and thus forbidden transitions are most prominent in this direction. No attempt was made to determine experimentally the hyperfine splittings due to forbidden transitions since the information normally obtained from them, the relative sign of the hyperfine tensor components, can be readily gotten from the high-temperature spectra.

(*b*) *ND_3Cl Center.* The deuterated form of the center is expected to show hyperfine spectra due only to the Cl and N nuclei, with unresolved deuteron transitions contributing to an enhanced linewidth. This is due to the small D hyperfine interaction, reduced by the factor $\mu_D I_H/\mu_H I_D=1/6.514$ from that of H (for an identical electronic configuration), and the increased number of hyperfine transitions because of the larger nuclear spin, $I=1$. This result is seen in the ND_3Cl spectrum of Fig. 2.

Line positions were fitted to the spin Hamiltonian of Eq. (1), omitting the nuclear Zeeman term. A computer simulation of the spectra, using the parameters given in Table II, produced an excellent fit to the recorded spectra for the mangetic field oriented along the ⟨111⟩, ⟨110⟩, and ⟨100⟩ directions; the value of the D interaction was obtained from the H-interaction parameters for NH_3Cl in the manner prescribed above. The values obtained for the Cl and N hyperfine tensors do not differ greatly from those obtained in the undeuterated case. We infer that the defect configuration does not change much under deuteration.

(c) *NH_3Br Center.* The NH_3Br defect center was found to be aligned along cubic unit cell body diagonals within experimental error ($\pm 1°$) despite the distortions of the crystal structure previously discussed. The EPR spectrum for the magnetic field aligned along a $\langle 111 \rangle$ direction is shown in Fig. 6. There are two Br isotopes of spin $\frac{3}{2}$ each, Br^{79} and Br^{81}, with magnetic moments of 2.0991 and 2.2626 μ_N, respectively, and nearly equal abundances. The dominance of the bromine hyperfine interaction, and the fortuitous equivalence of the N splitting to the separation of the $m_I=\frac{3}{2}$ transitions for the two Br isotopes, affords a better view of the individual splittings than in the case of NH_3Cl.

EPR transitions were fitted to the spin Hamiltonian

$$\mathcal{H}=g_{\parallel}\mu_B H_z S_z+g_{\perp}\mu_B(H_x S_x+H_y S_y)$$
$$+\mathbf{S}\cdot\sum \mathbf{A}_i\cdot\mathbf{I}_i+Q_{Br}'[I_z^2-\tfrac{1}{3}I(I+1)], \quad (10)$$

where Q_{Br}' is related to the Br nuclear quadrupole moment in the usual way.[22] Again, the angular dependence of the $\Delta M_S=\pm 1$, $\Delta m_I=0$ transitions was taken to second order,[16] neglecting cross terms of the order of $0.74 m_i m_j$ for $\langle 100 \rangle$ directions. The resulting spin Hamiltonian constants are given in Table II. H splittings were resolved only for the field along, or near, the N—Br bond direction, where the three H interactions are equivalent. Forbidden $\Delta m_I=\pm 1, \pm 2$ transitions due to the quadrupole term were not observed.

The asymmetry of the [100] spectrum, induced by the large Br nuclear-quadrupole moment, is readily seen in Fig. 2. The low field line is seen to be split into a quartet of lines resulting from the Br isotopic splitting combined with the N interaction of approximately equal magnitude, as in Fig. 6. The H interactions, inequivalent for this orientation, contribute to the linewidth. The gradual transition from the quartet to a barely resolved doublet structure in the direction of higher fields is caused by unequal quadrupole moments for the Br isotopes: $Q'(Br^{81})/Q'(Br^{79})=0.28/0.34$.

2. *180°K EPR Spectra*

EPR spectra from the NH_3Cl and ND_3Cl defect centers were observed to change reversibly as the temperature was cycled through the interval 77–180°K. Individual hyperfine transitions broadened rapidly in the interval 80–110°K, and the spectrum was essentially a broad singlet up to 150°K. Beyond this temperature an entirely new spectrum emerged, as shown in Fig. 7 for NH_3Cl. No change of this type was observed in the spectra of the NH_3Br center, although there was an increase in hyperfine linewidth with temperature. Each center annihilated above this range in temperature, disappearing rapidly in the interval 220–245°K.

[22] W. Low, in *Solid State Physics*, edited by F. Seitz and D. Turnbull (Academic Press Inc., New York, 1960), Suppl. 2.

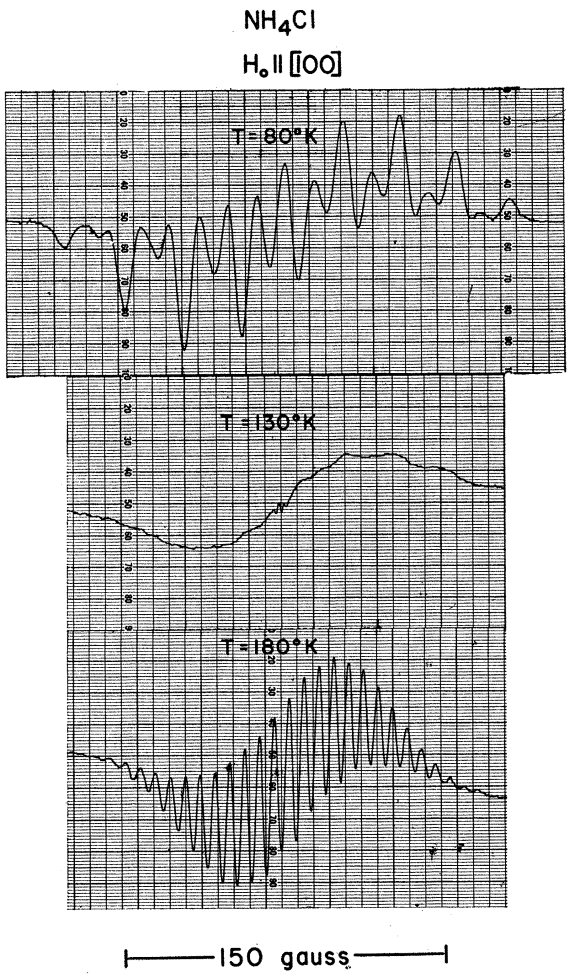

FIG. 7. Temperature dependence of the NH_3Cl spectrum.

The temperature dependence of the NH_3Cl spectrum suggests some kind of thermally activated reorientation of the defect. For an arbitrary direction of the applied field, the g factor and hyperfine interactions of the defect will change abruptly for each movement it makes. If the experimental apparatus is tuned to a particular hyperfine transition, the defect is alternately brought into resonance and out as it performs a random reorientation, leading to lifetime broadening of the hyperfine lines as the time spent in the resonance condition decreases. Experimentally, line broadening occurs when the temperature is such that the reorientation rate becomes as large as the low-temperature linewidth, about 10^7 sec^{-1}. Further increasing the temperature, and hence the reorientation rate, leads to a new motionally narrowed hyperfine spectrum which is the result of averaging the g tensor and hyperfine tensor components.

Of the two likely types of movement for the NH_3Cl defect, a threefold rotation about the N—Cl bond or a reorientation of the NH_3^+ ion and reformation of the N—Cl bond with a different Cl ion, only the latter is consistent with the high-temperature data. We interpret

the 180°K spectrum in Fig. 7 as follows. The large number of equally spaced lines with a Gaussian distribution of intensities must originate from equal coupling of the unpaired electron to several Cl nuclei. The line spacing should then be a measure of the reduction, from the 77°K case, of the coupling to the individual Cl nuclei. For this field orientation (**H**‖[100]), the measured separation of 6.9±0.1 G is exactly one-fourth the splitting due to the Cl^{35} hyperfine interactions in the 77°K case (27.5 G, Table I). The 180°K spectrum may thus be interpreted as arising from an unpaired electron, with a rapidly reorienting NH_3^+ group, interacting equally with *four* Cl nuclei.

The angular dependence of the 180°K EPR spectrum was found to have cubic symmetry. The anisotropy of the spectrum could be ascribed entirely to the Cl hyperfine interaction; N and H hyperfine interactions appeared to be isotropic. Complete averaging of the N and H hyperfine tensors could only be attained if the four Cl ions in the high-temperature form of the defect were tetrahedrally arranged around the reorienting NH_3^+ group, as shown in Fig. 3.

Rough values for the hyperfine tensor elements of the reorienting defect were obtained in the following manner, as suggested by the above model: We assume (1) the Cl hyperfine tensor elements are one-fourth those obtained at 77°K; (2) the N and H hyperfine couplings are isotropic ($\bar{A}_N$ and $\bar{A}_H$), and equal to one-third the trace of the respective 77°K tensors, $\bar{A}_i = \frac{1}{3}\mathrm{Tr}\mathbf{A}_i$. It is assumed that the reorienting NH_3^+ group does not distort appreciably from the 77°K configuration, and consequently the trace of each hyperfine tensor is invariant over this temperature interval. We ignore the signs of the N and H diagonal hyperfine tensor elements, since they do not affect the EPR splittings, and assume only that the elements in each set have the same relative sign. Then $\bar{A}_N = 21.5 \pm 2.9$ G and $\bar{A}_H = 23.3 \pm 2.3$ G. In constructing the expected 180°K EPR spectrum, the different isotopic combinations in a group of four Cl nuclei must be considered:

Comb.:	$4Cl^{35}$;	$(3Cl^{35})(Cl^{37})$;	$(2Cl^{35})(2Cl^{37})$;	$(Cl^{35})(3Cl^{37})$;	$4Cl^{37}$;
Rel. prob.:	81;	108;	54;	12;	1.

For the particular case of **H**‖[100], identical Cl isotopes have equivalent hyperfine interactions. For other field directions, the inequivalence of even the identical Cl isotopes produces an extremely large number of transitions and an almost unresolved hyperfine spectrum results. A computer simulation of the [100] spectrum with the above values produced a rough fit to the data. By successive approximations, an excellent fit was obtained with the following values: $A_{Cl35}(\mathbf{H}\|[100]) = 6.91 \pm 0.3$ G, $\bar{A}_N = 20.5 \pm 1.5$ G, $\bar{A}_H = 21.0 \pm 1.5$ G. The differences, $\Delta\bar{A}_N = 1$ G, $\Delta\bar{A}_H = 2.3$ G, between these values and the ones initially assumed are less than the minimum expected differences if one of the elements in the N and H hyperfine tensors had an opposite sign, $\Delta\bar{A}_N = 5.3$ G, $\Delta\bar{A}_H = 3.2$ G; this justifies the assumption of equal signs for each set of hyperfine tensor elements. The approximate equality of $\bar{A}_N$ and $\bar{A}_H$, and the fact that they are almost an exact multiple of $A_{Cl^{35}}$, is the reason for the fairly well-resolved [100] spectrum.

We may use the hyperfine couplings obtained above from a computer simulation of 180°K spectra to recalculate the 77°K hyperfine tensor elements, still assuming the configuration of the reorienting NH_3^+ does not distort over this temperature interval. The results are presented in Table II. Only the perpendicular elements for the Cl and N interactions were changed, since they are in greater estimated error; the parallel elements were kept constant. The correction to the H hyperfine tensor was made by uniformly reducing only A(H) and C(H) since B(H) is strongly dependent on the **H**‖[111] measurement and hence in little error.

A similar temperature dependence is observed for the ND_3Cl center except that hyperfine structure is scarcely resolved in the high-temperature regime because of the effects of the small interaction with the D nuclei and their additional transitions. The general features of the spectra are completely explained by extrapolation from the NH_3Cl results.

Ordering of NH_4^+ ions has been shown to be very largely caused by octupole-octupole interaction terms in a multipole expansion of Coulombic forces between nearest NH_4^+ neighbors, assuming a nearly unit charge evenly distributed on the hydrogen atoms.[23] This same interaction is evidently responsible for constraining the reorienting NH_3^+ group to bond to only four of the eight surrounding Cl^-. The tetrahedral NH_3Cl molecule will be in a position of minimum electrostatic energy when it is oriented similarly to the surrounding NH_4^+ tetrahedra. On this basis we exclude the possibility in which the defect orientation differs from that of Fig. 3 by a 60° rotation about the N—Cl bond. Other positions of minimum interaction energy occur when the NH_3^+ group is coupled to Cl^- ions which are on connecting face diagonals of the unit cell (solid circles in Fig. 3). The reorienting NH_3^+ presumably alternately couples only to these four Cl^- in the high-temperature form of the defect.

Estimates of the correlation time τ for the reorientation process were obtained for several temperatures by measuring the change of hyperfine linewidth in the

[23] C. W. Garland and J. S. Jones, J. Chem. Phys. 41, 1165 (1964).

temperature region of motional effects.[24] These measurements were severely hampered by the overlapping of transitions and the lack of a reference transition unaffected by the reorientational motion. The data were found to roughly fit the Arrhenius relation

$$1/\tau = \nu_0 e^{-E/kT}, \qquad (11)$$

with an activation energy within the range $E=0.04$–0.08 eV. For comparison, the activation energy for rotation of the NH_4^+ group in NH_4Cl has been measured to be 0.206 eV.[25] This suggests that the value for NH_3Cl is rather low for reorientation by rotation of the NH_3^+ group.

There is an alternative reorientational mechanism, which may have a lower activation energy than rotation. The N and one H could move through a {110} plane, breaking and reestablishing the N—Cl bond with a different Cl. In Fig. 3 is shown, in dashed circles, the result of one such reorientation for the NH_3Cl defect in which the NH_3 group moves to the position of its mirror image in the $(\bar{1}10)$ plane. The N atom moves about 1.5 Å in this process. A supporting feature of the mechanism is that the N atom is directed only to the tetrahedrally located Cl^- ions which are part of the high-temperature form of the defect. This is similar to bond switching reorientation processes, which generally have been found to have activation energies within the range reported here.[26,27]

Research on the kinetics of the reorientational motion is continuing, and will be fully reported in a forthcoming publication.[7]

3. *Optical Absorption Spectra*

Figure 8 shows the optical absorption spectra[28] of an irradiated NH_4Cl single crystal at 15°K before (a) and after (b) optically bleaching within the 790-nm band to remove the $V_K(Cl_2^-)$ center. About 75% of the initial uv band is due to the $^2\Sigma_g^+ \leftarrow {}^2\Sigma_u^+$ transition of the V_K center at 385 nm. The entire band at 790 nm is due to the $^2\Pi_g \leftarrow {}^2\Sigma_u^+$ transition of the V_K center.[3] The band labelled *b* at 375 nm (3.31 eV), with 1.0-eV half-width, is ascribed to the NH_3Cl center.

Polarized optical bleaching experiments[29] were conducted on the 375-nm band to determine if the center could be selectively oriented. No dichroism was produced in this band after intense irradiation with [001]-, [011]-, and [111]-polarized light in the absorption band. Similarly, it was not possible to increase or diminish the population of any of the ⟨111⟩-oriented NH_3Cl centers, when viewed by EPR, by appropriately polarized optical bleaching of the sample *in situ*. Continuous and pulsed thermal annealing experiments showed a correspondence between the decrease in magnitude of the 375-nm optical absorption band and the EPR signal due to the NH_3Cl center.

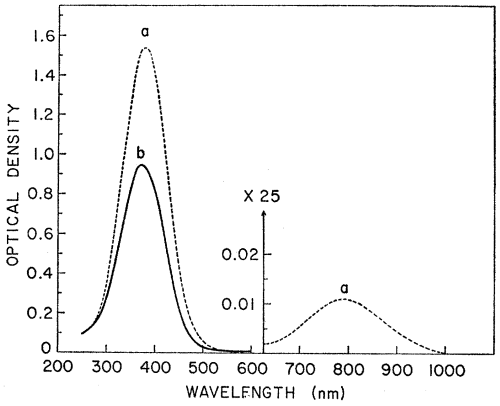

FIG. 8. Optical absorption spectra of an irradiated NH_4Cl single crystal at low temperature before (a) and after (b) optically bleaching.

Similar experiments were performed on an irradiated NH_4Br single crystal, which has an optical absorption spectrum qualitatively similar to Fig. 8. An optical absorption band at 395 nm (3.14 eV), with 1.0-eV half-width, was found to decrease in amplitude roughly in correspondence with the NH_3Br EPR spectrum after thermal annealing.

The experiments described are consistent with the identification of the 3.31 eV, 3.14 eV optical absorption bands as due to the NH_3Cl, NH_3Br centers, respectively. These transitions probably would occur between the σ-bonding and σ-antibonding molecular orbitals shown in the energy-level scheme of Fig. 11, as discussed in the following section.

ANALYSIS

1. *Electronic Ground State*

An approximate description of the NH_3X electronic wave functions can be found by using a linear combination of atomic orbitals based on known NH_3^+ molecular orbitals and X^- atomic orbitals. Self-consistent-field (SCF) molecular orbitals, based on Hartree-Fock wave functions, have been constructed by Lorquet and Lefebvre-Brion for the NH_3^+ radical in both the planar

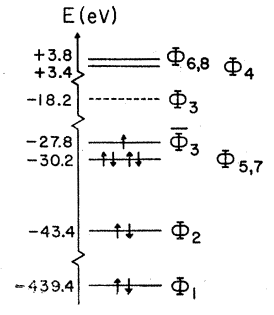

FIG. 9. Energy-level scheme for NH_3^+ (Ref. 21). The difference between Φ_{III} and $\bar{\Phi}_{III}$ is the electronic exchange interaction: $\bar{E}_3 = E_3 - \frac{1}{2}J_{33}$.

[24] H. S. Gutowsky and A. Saika, J. Chem. Phys. **21**, 1688 (1953).
[25] E. M. Purcell, Physica **17**, 738 (1947).
[26] B. Dischler, A. Rauber, and J. Schneider, Phys. Status Solidi **6**, 507 (1964).
[27] G. D. Watkins and J. W. Corbett, Phys. Rev. **134**, A1359 (1964).
[28] From data taken by M. J. Marrone of this laboratory.
[29] Performed in collaboration with M. J. Marrone.

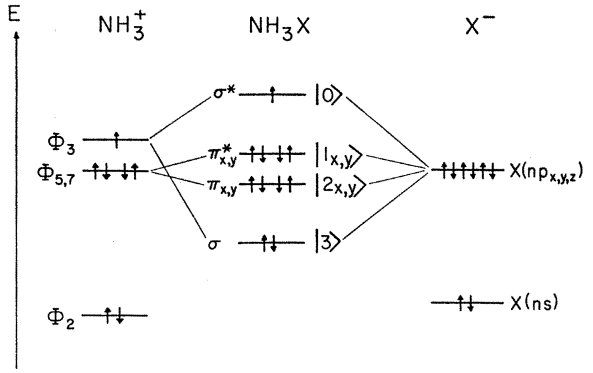

FIG. 10. Formation of NH_3Cl, NH_3Br molecular orbitals.

and pyrimidal configurations,[30] in an extension of earlier studies by Kaplan on the ammonia molecule.[31] Giacometti and Nordio[32] performed a configuration-interaction calculation using these molecular orbitals and obtained isotropic coupling constants $\bar{A}_N$ and $\bar{A}_H$ for NH_3^+ in good agreement with experiment.[11] The energy-level scheme for NH_3^+, in the notation of Lorquet and Lefebvre-Brion, is shown with filled orbitals in Fig. 9. The values shown are extrapolated between the planar and pyrimidal cases for the small (3°) distortion from the planar configuration found for NH_2Cl (a larger distortion must occur for NH_3Br, but the qualitative aspects of the resulting molecular-orbital scheme will remain the same). The molecular orbitals are

$$\begin{aligned}
\Phi_1&=+\mathrm{N}(1s),\\
\Phi_2&=+0.025\mathrm{N}(1s)+0.806\mathrm{N}(2s)\\
&\quad+0.033\mathrm{N}(2p_z)-0.234\mathrm{H}_0,\\
\Phi_3&=+0.003\mathrm{N}(1s)-0.066\mathrm{N}(2s)\\
&\quad+0.985\mathrm{N}(2p_z)-0.033\mathrm{H}_0,\\
\Phi_4&=-0.151\mathrm{N}(1s)+1.314\mathrm{N}(2s)\\
&\quad+0.080\mathrm{N}(2p_z)+1.545\mathrm{H}_0,\\
\Phi_{5,7}&=+0.756\mathrm{N}(2p_{x,y})+0.326\mathrm{H}_{x,y},\\
\Phi_{6,8}&=-1.087\mathrm{N}(2p_{x,y})+1.282\mathrm{H}_{x,y},
\end{aligned}\tag{12}$$

where H_0, H_x, and H_y are normalized linear combinations of atomic hydrogen orbitals:

$$\begin{aligned}
\mathrm{H}_0&=0.46[\mathrm{H}_a(1s)+\mathrm{H}_b(1s)+\mathrm{H}_c(1s)],\\
\mathrm{H}_x&=0.96[\mathrm{H}_a(1s)-\tfrac{1}{2}(\mathrm{H}_b(1s)+\mathrm{H}_c(1s))],\\
\mathrm{H}_y&=0.83[\mathrm{H}_b(1s)-\mathrm{H}_c(1s)].
\end{aligned}\tag{13}$$

The multiplicative constants were calculated for the N—H bond length in NH_4^+ of 1.03 Å.

The formation of molecular orbitals from NH_3^+ and Cl^- or Br^- orbitals of appropriate symmetry is shown schematically in Fig. 10, with the expected order of energy levels (not to scale). It is possible that the state $|3\rangle$ lies above or between the states $|2_{x,y}\rangle$ and $|1_{x,y}\rangle$, depending on the relative energies of the uncorrelated NH_3^+ and X^- ions. Guided by the forms of Φ_3 and $\Phi_{5,7}$ in Eqs. (12), the NH_3X wave functions can be written as linear combinations of atomic orbitals (LCAO's) with undetermined coefficients:

$$\begin{aligned}
|0\rangle&=-a_N\mathrm{N}(2s)+b_N\mathrm{N}(2p_z)-a_H\mathrm{H}_0\\
&\quad+a_X X(ns)+b_X X(np_z),\\
|1_{x,y}\rangle&=+d_1\mathrm{N}(2p_{x,y})+e_1\mathrm{H}_{x,y}-f_1X(np_{x,y}),\\
|2_{x,y}\rangle&=+d_2\mathrm{N}(2p_{x,y})+e_2\mathrm{H}_{x,y}+f_2X(np_{x,y}),\\
|3\rangle&=-a_N'\mathrm{N}(2s)+b_N'\mathrm{N}(2p_z)-a_H'\mathrm{H}_0\\
&\quad-a_X'X(ns)-b_X'X(np_z),
\end{aligned}\tag{14}$$

where we have added halogen ns orbitals to conform to the experimental hyperfine data. We have neglected, for ease of computation, contributions from halogen $(n+1)s$ orbitals, but have compensated somewhat for this by including $X^-(ns)$ orbitals in the final comparison. In the ground state $|0\rangle$, the unpaired electron occupies an antibonding σ orbital and the state is $^2\Sigma$. Both the bonding and antibonding π orbitals remain degenerate in an environment of C_{3v} symmetry.

The molecular orbital picture and its accompanying energy-level scheme presented here, along with specific energy differences to be given later, are very similar to those of mixed V_K centers XY^-.[33–36] Similarities can also be seen in the physical model in which the electronegative NH_3^+ group corresponds to a halogen atom; it has one electron missing from its "closed-shell" configuration NH_3^0. We adopt a hole-type description of the center in accord with this viewpoint. Spin-orbit coupling, now of negative sign, causes some admixture of the bonding and antibonding π orbitals into the ground state, producing the observed g shift. The transition giving rise to the optical absorption, shown in Fig. 11, is, as in the V_K center, due to a transference of unpaired electron density along the N—X bond axis. The transition moment is expected to be large for light polarized along this direction. Optical absorption due to transitions to the Π levels is expected to be small, and none was in fact found.

2. *g*-Tensor Components

Treating the spin-orbit coupling $\lambda\mathbf{L}\cdot\mathbf{S}$ as a perturbation, the modified ground-state wave functions are calculated to be

$$\begin{aligned}
|+\rangle&=[1-\xi_0^2][|0\alpha\rangle+\xi_1|1_x\beta\rangle+i\xi_1|1_y\beta\rangle\\
&\quad+\xi_2|2_x\beta\rangle+i\xi_2|2_y\beta\rangle],\\
|-\rangle&=[1-\xi_0^2][|0\beta\rangle-\xi_1|1_x\alpha\rangle+i\xi_1|1_y\alpha\rangle\\
&\quad-\xi_2|2_x\alpha\rangle+i\xi_2|2_y\alpha\rangle],
\end{aligned}\tag{15}$$

[30] J. C. Lorquet and H. Lefebvre-Brion, J. Chim. Phys. **57**, 85 (1960).
[31] H. Kaplan, J. Chem. Phys. **26**, 1704 (1957).
[32] G. Giacometti and P. L. Nordio, Mol. Phys. **6**, 301 (1963).
[33] D. Schoemaker, Phys. Rev. **149**, 693 (1966).
[34] J. W. Wilkins and J. R. Gabriel, Phys. Rev. **132**, 1950 (1963).
[35] W. Dreybrodt and D. Silber, Phys. Status Solidi **16**, 215 (1966).
[36] M. L. Meistrich and L. S. Goldberg, Solid State Commun. **4**, 469 (1966).

where α and β are the two spin states, and the coefficients are

$$\begin{aligned}&\xi_1\cong(b_N d_1\lambda_N - b_X f_1\lambda_X)/2\Delta_1,\\&\xi_2\cong(b_N d_2\lambda_N + b_X f_2\lambda_X)/2\Delta_2,\\1-\xi_0^2&=(1+2\xi_1^2+2\xi_2^2)^{-1/2}\\&\cong 1-(b_X\lambda_X/2)^2[(f_1/\Delta_1)^2+(f_2/\Delta_2)^2].\end{aligned}\tag{16}$$

Δ_1 and Δ_2 are the energy differences of the $|1_{x,y}\rangle$ and $|2_{x,y}\rangle$ states from the ground state, as shown in Fig. 11. We have dropped terms in λ_N^2, since $\lambda_N^2\ll\lambda_X^2$, and have assumed vanishing overlap integrals,

$$\langle N(2p_{x,y})|X(np_{x,y})\rangle=0.$$

Using standard techniques, and expanding to second order in λ/Δ, we obtain the following results for the g shifts:

$$\begin{aligned}\Delta g_{\parallel}=g_{\parallel}-g_e&=-(b_X\lambda_X)^2[(f_1/\Delta_1)^2(2-d_1^2-f_1^2)\\&\quad+(f_2/\Delta_2)^2(2-d_2^2-f_2^2)],\\\Delta g_{\perp}=g_{\perp}-g_e&=-2b_N^2\lambda_N[d_1^2/\Delta_1+d_2^2/\Delta_2]\\&\quad-2b_X^2\lambda_X[f_1^2/\Delta_1+f_2^2/\Delta_2]+2b_N b_X(\lambda_N+\lambda_X)\\&\quad\times[d_1f_1/\Delta_1-d_2f_2/\Delta_2]\\&\quad-(b_X\lambda_X)^2[(f_1/\Delta_1)^2+(f_2/\Delta_2)^2],\end{aligned}\tag{17}$$

where $g_e=2.0023$. There are too many unknown quantities for a solution of these equations. However, some rough approximations can be made to see if the resulting simple relations predict qualitatively correct behavior: $f_1^2+f_2^2\approx1$; $d_1^2+d_2^2\approx1$; $d_1f_1-d_2f_2\approx0$. Equations (17) reduce to

$$\Delta g_{\parallel}\approx-(b_X\lambda_X/\Delta)^2,\tag{18a}$$

$$\Delta g_{\perp}\approx-2b_X^2\lambda_X/\Delta,\tag{18b}$$

where Δ is the mean of the energy separations Δ_1 and Δ_2 (positive quantities). Equations (18) show the correct signs for the g shifts. Combining these relations, we obtain $\Delta g_{\perp}\approx-2b_X(|\Delta g_{\parallel}|)^{1/2}$; using values for $\Delta g_{\parallel}$ and b_X given in Tables II and IV, we find $\Delta g_{\perp}(NH_3Cl)\approx-0.0180$ and $\Delta g_{\perp}(NH_3Br)\approx-0.1179$. These predicted values are higher by factors of 3 and 2, respectively, than the quantities given in Table II, but the correspondence is satisfactory considering the approximations made. Equations (18) may each be solved for Δ. Taking $\lambda_{Cl}=-0.073$ eV, $\lambda_{Br}=-0.305$ eV,[37] we find $\Delta=1.7$(a), 5.6(b) eV for NH_3Cl and $\Delta=2.7$(a), 5.7(b) eV for NH_3Br. The lower value for Δ is believed to be more nearly correct in each case, since it is obtained from the relation for $\Delta g_{\parallel}$ which is based on more valid approximations.

3. *Hyperfine Tensor Components*

A relation is obtained between the hyperfine tensor components of the spin Hamiltonian and the coefficients

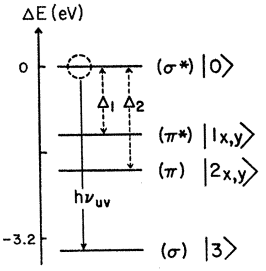

FIG. 11. Energy-level scheme for NH_3X, showing observed optical transition.

of the wave function by averaging the hyperfine interactions,

$$\mathcal{H}^{HF}=\sum_i g_e\mu_B\frac{\mu_i}{I_i}\left[\frac{(\mathbf{L}_i-\mathbf{S}_i)\cdot\mathbf{I}_i}{r_i^3}+\frac{3(\mathbf{r}_i\cdot\mathbf{S})(\mathbf{r}_i\cdot\mathbf{I}_i)}{r_i^5}+\frac{8\pi}{3}\mathbf{S}\cdot\mathbf{I}_i\delta(\mathbf{r}_i)\right],\tag{19}$$

over the orbital part of the ground-state wave function [Eq. (15)]. There is an additional contribution to the usual equations[38] due to the $\mathbf{L}_i\cdot\mathbf{I}_i/r_i^3$ term acting on admixtures of excited states into the ground-state wave function. The result of the calculation is, to first order,[33]

$$\begin{aligned}A_{\parallel,i}&=A_i+2B_i,\\A_{\perp,i}&=A_i-B_i+\tfrac{5}{2}\Delta g_{\perp}B_i,\end{aligned}\tag{20}$$

where

$$\begin{aligned}A_i&=(8\pi/3)(\mu_i/I_i)a_i^2|\Psi_{ns}(0)|^2,\\B_i&=\tfrac{2}{5}(\mu_i/I_i)b_i^2\langle r_i^{-3}\rangle_{np}.\end{aligned}$$

Values of $|\Psi_{ns}(0)|^2$ and $\langle r^{-3}\rangle_{np}$ for the different atoms, calculated for the most part from the analytic Hartree-Fock wave functions obtained by Watson and Freeman,[39] are given in Table III. The mean of these values for X and X^- was used in subsequent computations. Using the EPR data in Table II, the spin densities a_i^2 and b_i^2 in the ns and np atomic orbitals were calculated from Eqs. (20). The results are shown in Table IV.

TABLE III. Values of $\langle r^{-3}\rangle_{np}$ and $|\Psi_{ns}(0)|^2$, in units of 10^{24} cm^{-3}.

n	Nucleus	$\lvert\Psi_{ns}(0)\rvert^2$	$\langle r^{-3}\rangle_{np}$
1	H^1	2.14[a]	...
2	N^{14}	32.22[a]	20.95[a]
3	Cl^{35}	71.90[b]	45.32[b]
3	$(Cl^{35})^-$	68.14[b]	38.93[b]
4	Br^{79}	131.14[b]	80.22[b]
4	$(Br^{79})^-$	124.29[b]	69.20[b]

[a] J. R. Morton, Chem. Rev. 64, 453 (1964).
[b] R. E. Watson and A. J. Freeman, Phys. Rev. 123, 521 (1961); 124, 1117 (1961).

[37] M. Blume and R. E. Watson, Proc. Roy. Soc. (London) A271, 565 (1963).

[38] C. P. Slichter, *Principles of Magnetic Resonance* (Harper and Row, New York, 1963), Sec. 7.3.

[39] R. E. Watson and A. J. Freeman, Phys. Rev. 123, 521 (1961); 124, 1117 (1961).

TABLE IV. Spin densities, a_i^2 and b_i^2, in s- and p-type atomic orbitals on NH_3X nuclei.

	A_i	B_i	a_i^2	b_i^2	$a_i^2+b_i^2$
			NH_3Cl		
Cl^{35}	23.3	10.0	0.014	0.214	0.229
N	21.4	12.6	0.039	0.736	0.776
H	−23.3	···	−0.046		−0.046
			NH_3Br		
Br^{79}	202.1	112.2	0.027	0.531	0.559
N	40.7	5.4	0.074	0.318	0.392

Some features of the results in Table IV are the following:

(a) The NH_3Cl molecule has a high ionic character and may more accurately be written as $NH_3^+Cl^-$, with the hole density lying mainly in the NH_3^+ group. There is a more uniform distribution of hole density on the NH_3Br molecule, indicating a greater amount of covalency between the N and Br. This implies greater strength of the N—X bond in NH_3Br, which is consistent with the fact that motional effects due to a reorienting NH_3^+ group are not observed.

(b) The s-type admixture into the nitrogen wave function is proportionately much greater in NH_3Br than in NH_3Cl. Thus, in NH_3Br, there is a greater tendency toward sp^3 (tetrahedral) hybridization of the nitrogen orbitals with stronger covalent bonding, already inferred, to the bromine. Assuming the departure of the X—N—H bond angle from the planar configuration is a linear function of the amount of sp^3 hybridization of the nitrogen orbitals, we find

$$(\psi-90°)=3(19.5°)a_N^2/b_N^2.$$

From the data in Table IV we obtain $\psi(NH_3Cl)=93°$, in excellent agreement with the previous result, and $\psi(NH_3Br)=104°$.

DISCUSSION

The NH_3X center is probably formed by the removal of H° from NH_4^+ by the incident ionizing radiation, with subsequent bonding of NH_3^+ to X^- along a ⟨111⟩ direction. The paramagnetic resonance spectrum for H° was not observed. It seems likely that H° either directly escapes from the lattice or moves through the crystal, even at the lowest irradiation temperatures of about 30°K, and forms molecular H_2.

It has been shown that the NH_3X defect structure is in general similar to that of mixed V_K centers of the type XY^-. The energy-level scheme and optical transition energies are also quite similar. In the NH_3Cl center, NH_3^+ is a nearly planar group, loosely bonded to Cl^-, and alternately bonded to three other Cl^- in accordance with a reorientational mechanism which is influenced by the surrounding ordered NH_4^+ groups. In the NH_3Br center, the NH_3^+ group departs more from a planar configuration and there is stronger covalent bonding to a Br^-.

It has been noted that the ground state $|0\rangle$ of the NH_3Cl defect is largely ionic. From the orthogonality condition we infer that the excited state $|3\rangle$ taking part in the optical transition has a similar ionicity, with its electric dipole moment oriented in the opposite direction. This suggests that the optical transition energy might be in agreement with a formula derived from a simple electron transfer model,[40]

$$E=E_A-E_I+(2\alpha_M-1)e^2/R, \qquad (21)$$

where E_A is the electron affinity of $X°$, E_I the ionization energy of $NH_3°$, α_M the Madelung constant, and R the nearest-neighbor distance. The first two terms on the right-hand side of Eq. (21) represent the work done in removing an electron from X^- and then adding it to NH_3^+. The last term represents the energy expended in moving the electron through the Coulomb potential of the surrounding ions; the -1 takes into account the fact that there is a missing charge seen by the electron (at the position of the former X^-) when bringing it to the position of NH_3^+. It is assumed that NH_3^+ lies at the center of the unit cube. Using the following values: $E_A=3.61$ eV, $E_I=11.2$ eV, and $\alpha_M e^2/R=7.55$ eV, we obtain for the transition energy $E=3.2$ eV. This is in remarkably good agreement with the observed energy of 3.31 eV. The formula is less accurate when applied to the less ionic NH_3Br defect: From $E_A=3.36$ eV and $\alpha_M e^2/R=7.21$ eV we find $E=2.5$ eV, compared to the observed energy of 3.14 eV.

Both centers annihilate above 200°K within a 20° temperature interval just below the order-disorder transition temperature, and no resulting paramagnetic species are observed in EPR. Some likely processes leading to nonparamagnetic products are

1. $NH_3X+e^-\rightarrow NH_3°+X^-$;
2. $NH_3X\rightarrow NH_2X+H°$,
   $H°+H°\rightarrow H_2$,;
3. $NH_3X\rightarrow NH_2+HX$,
   $NH_2+NH_2\rightarrow N_2H_4$,;
4. $NH_3X\rightarrow NH_3°+X°$,
   $X°+X°\rightarrow X_2$.

The first process seems doubtful for the following reason. The V_K center is known to annihilate at about 150°K by recombining with a trapped electron, with no noticeable effect on the numbers of NH_3X centers present. If an electron-hole recombination process for NH_3X were to become favored only at an elevated temperature, there is then no evidence (from EPR or

[40] R. S. Knox, *Theory of Excitons* (Academic Press Inc., New York, 1963), Chap. 5. Although Eq. (21) does not work particularly well when applied to exciton absorption bands in alkali halides, it is more applicable to this case because of the localized nature of the defect.

optical spectra) for the existence of trapped electron centers, at this higher temperature, which could supply electrons in sufficient numbers. F centers are ruled out as a source of electrons since they are stable[2] up to 100°C and in any case their population relative to NH_3X is exceedingly small. It appears likely that annihilation occurs by some dissociation of the NH_3X molecule, illustrated by the latter three possibilities.

In each of the last three cases, one of the direct dissociation products is a paramagnetic species (H°, NH_2, X°) which is then required to combine with another to produce a stable nonparamagnetic molecule. The intermediate paramagnetic product must be able to diffuse swiftly through the lattice. For this reason, the second process appears most likely as the actual means of annihilation of NH_3X centers.

ACKNOWLEDGMENTS

The stimulating advice of M. N. Kabler throughout much of this work is gratefully acknowledged. The author is indebted to C. M. Marquardt for writing the computer programs, and to M. J. Marrone for the use of his optical absorption data. He would also like to acknowledge many informative discussions with M. H. Reilly and the continued interest and comments of C. C. Klick. Several suggestions by D. L. Griscom were incorporated in the final manuscript.

PHYSICAL REVIEW VOLUME 175, NUMBER 3 15 NOVEMBER 1968

Additive Coloration of Alkaline-Earth Chalcogenides*

EUGENE B. HENSLEY, WIRT C. WARD,† BRUCE P. JOHNSON,‡ AND ROGER L. KROES
Department of Physics, University of Missouri, Columbia, Missouri 65201
(Received 1 July 1968)

Procedures for the additive coloration of single crystals of the alkaline-earth chalcogenides are described. Both the coloring bombs and the two-section vacuum furnace are made of tantalum. Coloring temperatures used range from 1500 to 1900°C, with the pressure of the metallic vapor ranging up to several atmospheres.

I. INTRODUCTION

IN the additive coloring process, color centers are introduced into a solid by heating the crystals in a vapor of their metallic constituent. The literature pertaining to the color centers thus produced in the alkali halides is vast.[1] However, very few studies have been reported for similar studies in the alkaline-earth chalcogenides. Such studies are of great interest because the alkaline-earth chalcogenides may be regarded as divalent counterparts to the alkali halides. Sproull *et al.*[2–4] have identified and studied the F' centers (anion vacancies containing two electrons) in additively colored barium oxide crystals. Weber[5] reported color centers induced in magnesium oxide crystals by heating them in oxygen and in calcium and magnesium vapors. However, Soshea *et al.*[6] showed that the oxygen-induced color centers in Weber's work were due to impurities and cast doubt on Weber's interpretation of his metal-induced absorption bands. Studies of the optical absorption induced in several of the alkaline-earth oxides by various forms of irradiation have also been reported[6,7]; however, the complexity of the absorption spectra produced makes it difficult to identify the color centers responsible for the various observed bands.

In the present investigation, techniques have been developed for carrying out the additive coloring process at much higher temperatures than have hitherto been achieved. Using coloring temperatures as high as 1900°C, both F and F' centers, that is, anion vacancies containing one and two electrons, respectively, have been produced in calcium oxide[8] and strontium oxide[9] and F' centers have been produced in magnesium oxide.[10] These color centers have been studied both as a function of the coloring temperature and the pressure of the vapor of the metallic constituent.

The experimental technique used is an adaptation of the familiar double-furnace principles commonly employed in the additive coloration of the alkali halides.

* Work supported by the U. S. Office of Naval Research and the National Science Foundation.
† Present address: Department of Physics, Northern Arizona University, Flagstaff, Ariz.
‡ Present address: X-Ray Department, General Electric Company, Milwaukee, Wisc.
[1] J. H. Schulman and W. D. Compton, *Color Centers in Solids* (The Macmillan Co., New York, 1962).
[2] R. L. Sproull, R. S. Bever, and G. Libowitz, Phys. Rev. **92**, 77 (1953).
[3] W. C. Dash, Phys. Rev. **92**, 68 (1953).
[4] C. Timmer, J. Appl. Phys. **28**, 495 (1957).
[5] H. Weber, Physik **130**, 392 (1951).
[6] R. W. Soshea, A. J. Dekker, and J. P. Sturtz, J. Phys. Chem. Solids **5**, 23 (1958).
[7] Y. Chen and W. A. Sibley, Phys. Rev. **154**, 842 (1967).
[8] W. C. Ward and E. B. Hensley, following paper, Phys. Rev. **175**, 1230 (1968).
[9] B. P. Johnson and E. B. Hensley (to be published); see also Bull. Am. Phys. Soc. **12**, 411 (1967).
[10] K. L. Kroes and E. B. Hensley (to be published); see also Bull. Am. Phys. Soc. **13**, 420 (1968).